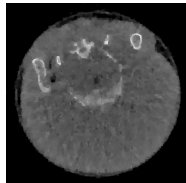
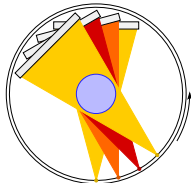
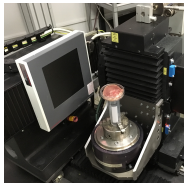


Structural Priors in Multi-Energy CT Reconstruction

Alexander Meaney, MSc

Computational Inverse Problems Research Group
Department of Mathematics and Statistics
University of Helsinki, Finland
alexander.meaney@helsinki.fi

Modern Challenges in Imaging
Tufts University, Medford, Massachusetts
5 August, 2019



Research team

Researcher Jussi Toivanen, PhD
University of Eastern Finland

PhD Student Alexander Meaney, MSc
University of Helsinki

Professor Ville Kolehmainen, PhD
University of Eastern Finland

PhD Student Mikael Juntunen, MSc
University of Oulu

Professor Samuli Siltanen, PhD
University of Helsinki

Outline

X-ray physics and imaging model in computed tomography

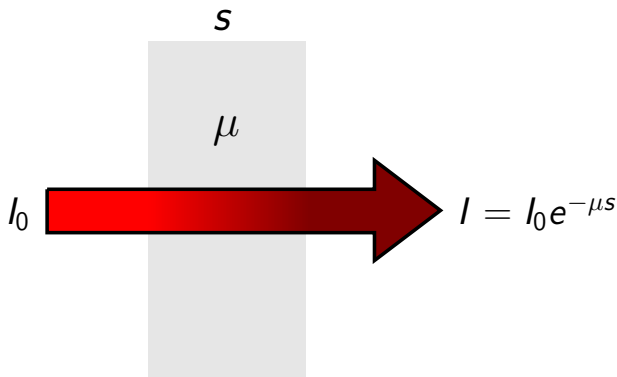
Material decomposition in multi-energy CT

Joint reconstruction in multi-energy CT

FIPS open datasets and Industrial Mathematics CT
Laboratory at the University of Helsinki

X-ray attenuation in matter

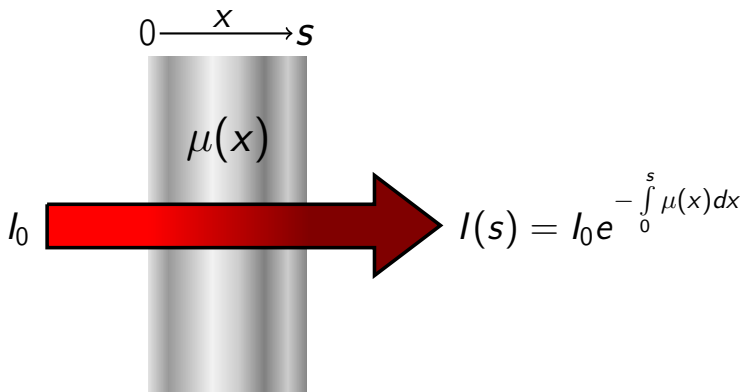
The attenuation of X-rays travelling through matter is described by *Lambert-Beer's Law*.



Here s is the thickness of the homogeneous medium and μ is the *linear attenuation coefficient*.

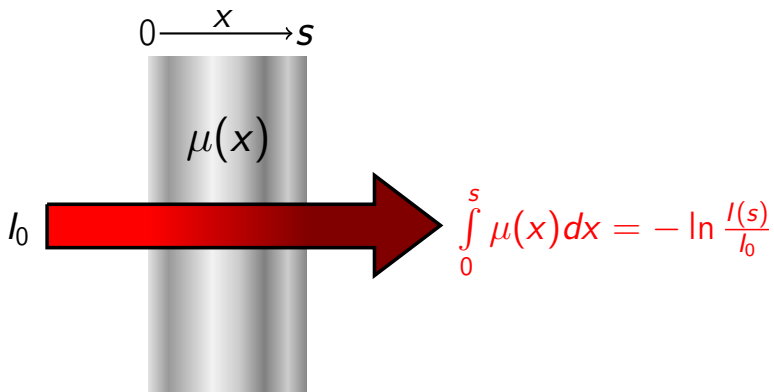
X-ray attenuation in matter

In the case of spatially varying attenuation, we must modify Lambert-Beer's Law.



X-ray attenuation in matter

Because we are especially interested in the spatial variation of μ , we usually emphasize the line integral.



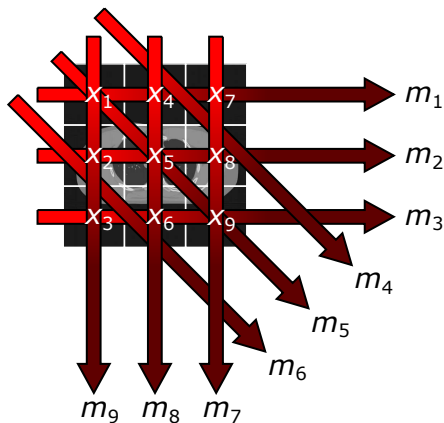
Discretized linear imaging model in computed tomography

We will model our measurements $m \in \mathbb{R}^k$ as

$$m = Ax + \varepsilon,$$

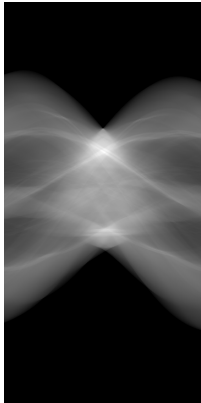
where $x \in \mathbb{R}^n$ is the discretized distribution of attenuation coefficients.

The forward model $A \in \mathbb{R}^{k \times n}$ is often called the *system matrix*.

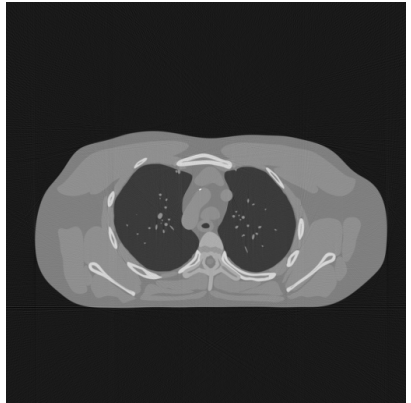


$$m_i = -\ln \frac{I_{\text{out}}}{I_0}$$

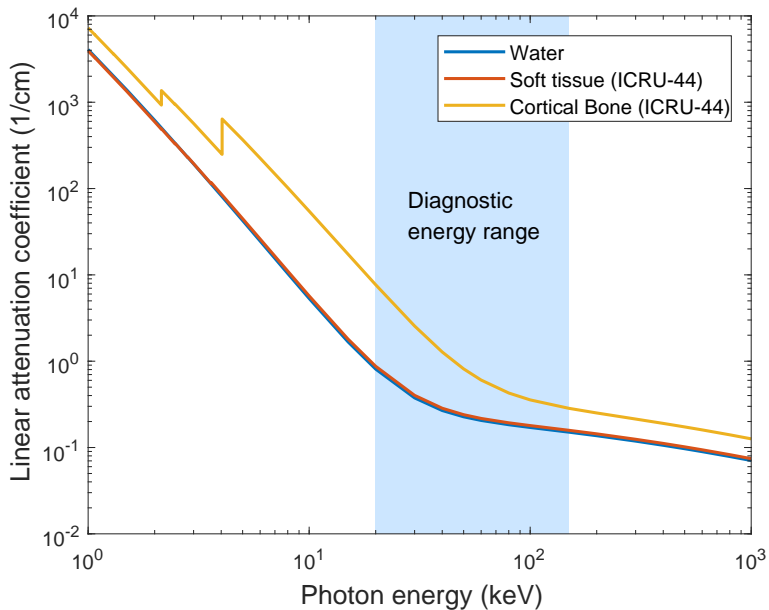
CT reconstruction: a problem already solved?



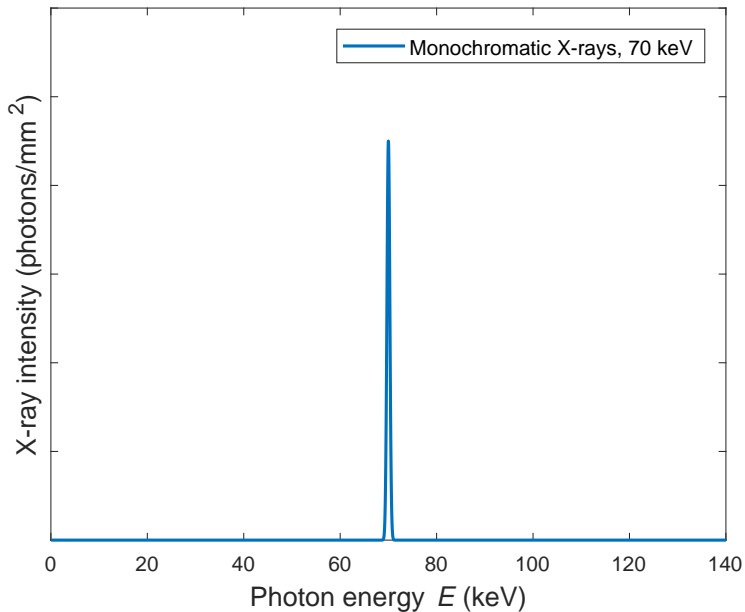
Reconstruction
algorithm



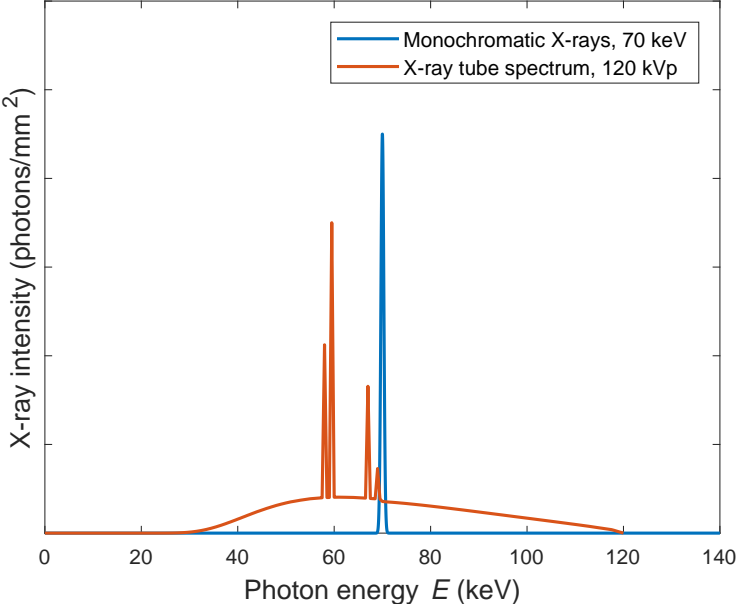
X-ray attenuation coefficients



Ideal, monochromatic X-ray spectrum



Energy spectrum of X-ray tube



Problems with Lambert-Beer's law

When imaging with polychromatic X-rays, we must also integrate across the source, *i.e.* X-ray tube, spectrum:

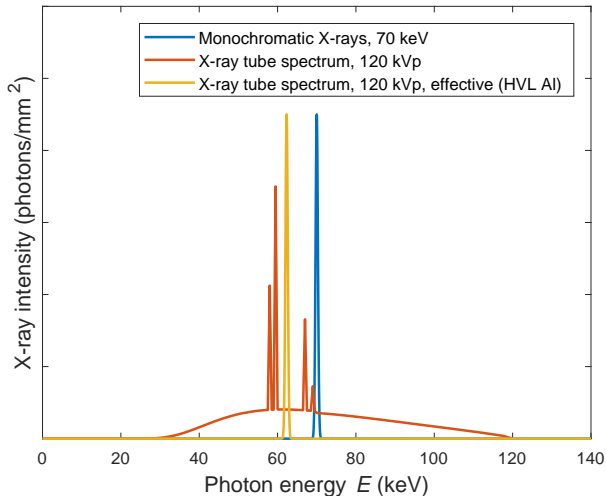
$$I(s) = \int_0^{E_{\max}} I_0(E) e^{-\int_0^s \mu(x,E) dx} dE.$$

This makes practical X-ray tomography an emphatically non-linear process. It also forces us to ask the following question:

What is the actual physical quantity we are trying to reconstruct?

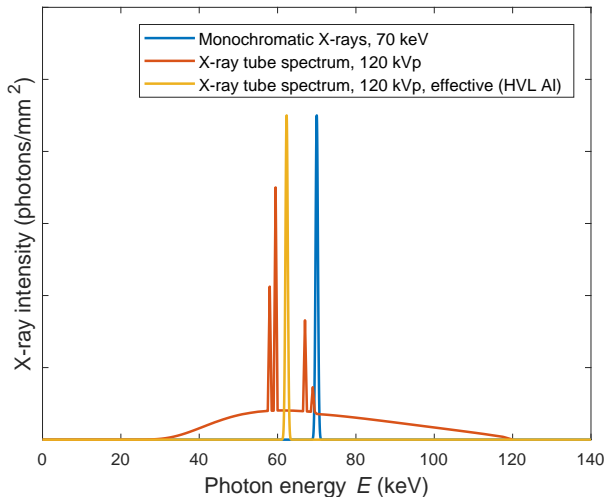
Problems with Lambert-Beer's law

One approach is to define an *effective X-ray energy* for which we are reconstructing the attenuation coefficients.



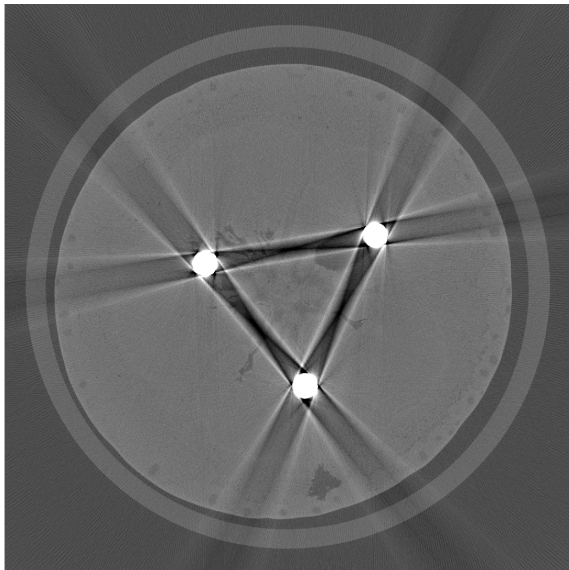
Problems with Lambert-Beer's law

One approach is to define an *effective X-ray energy* for which we are reconstructing the attenuation coefficients.



Be warned: this model does not make the underlying process any less nonlinear!

Using a linear model for a nonlinear process can lead serious issues



Metal artefacts in kumquat fruit with three inserted steel nails.

Outline

X-ray physics and imaging model in computed tomography

Material decomposition in multi-energy CT

Joint reconstruction in multi-energy CT

FIPS open datasets and Industrial Mathematics CT
Laboratory at the University of Helsinki

Why use multi-energy CT?

In computed tomography, there is not bijective relationship between the μ and the properties, *i.e.*, elemental composition and density, of the material.

For more precise information on the material composition, or **basis materials**, we need more data. For this, we can use *multi-energy CT* (MECT) or *dual energy CT* (DECT).

The aim is to compute a **material composition** and thus obtain **material specific reconstructions** for the different basis materials.

Material decomposition projection domain vs. image domain

Projection domain

Acquire projection images at
multiple energies



Convert projections into basis
materials



Reconstruct into basis
material images

Image domain

Acquire projection images at
multiple energies



Compute reconstructions at
each energy



Convert reconstructions into
basis material images

Material decomposition projection domain vs. image domain

Projection domain

Acquire projection images at
multiple energies



Convert projections into basis
materials



Reconstruct into basis
material images

Image domain

Acquire projection images at
multiple energies



Compute reconstructions at
each energy



Convert reconstructions into
basis material images

Material decomposition projection domain vs. image domain

Projection domain

Acquire projection images at
multiple energies



Convert projections into basis
materials



Reconstruct into basis
material images

Image domain

Acquire projection images at
multiple energies



Compute reconstructions at
each energy



Convert reconstructions into
basis material images

Material decomposition projection domain vs. image domain

Projection domain

Acquire projection images at
multiple energies



Convert projections into basis
materials



Reconstruct into basis
material images

Image domain

Acquire projection images at
multiple energies



Compute reconstructions at
each energy



Convert reconstructions into
basis material images

Material decomposition projection domain vs. image domain

Projection domain

Acquire projection images at
multiple energies



Convert projections into basis
materials



Reconstruct into basis
material images

Image domain

Acquire projection images at
multiple energies



Compute reconstructions at
each energy



Convert reconstructions into
basis material images

Material decomposition projection domain vs. image domain

Projection domain

Acquire projection images at
multiple energies



Convert projections into basis
materials



Reconstruct into basis
material images

Image domain

Acquire projection images at
multiple energies



Compute reconstructions at
each energy



Convert reconstructions into
basis material images

Material decomposition projection domain vs. image domain

Projection domain

Acquire projection images at
multiple energies



Convert projections into basis
materials



Reconstruct into basis
material images

Image domain

Acquire projection images at
multiple energies

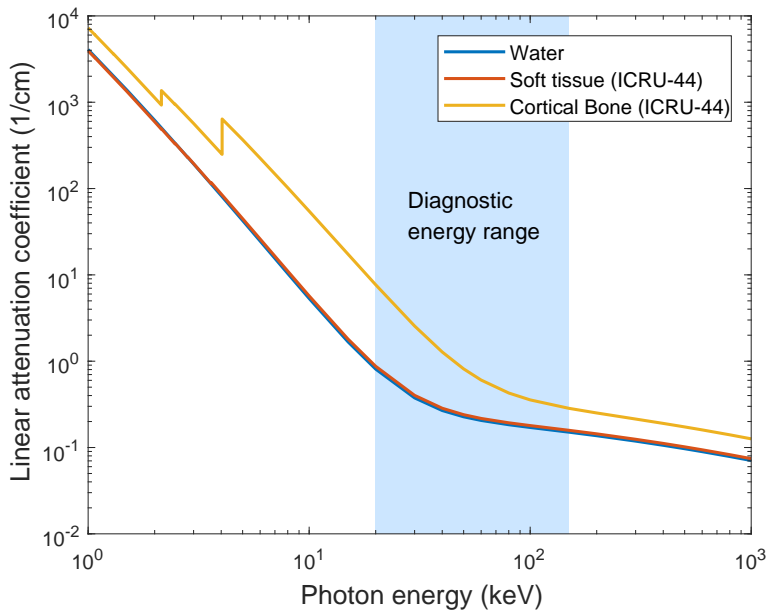


Compute reconstructions at
each energy



Convert reconstructions into
basis material images

X-ray attenuation coefficients



Generalized linear model of multi-energy CT in image space

We define the *mass attenuation coefficient* of a given material through the equation

$$\mu = \left(\frac{\mu}{\rho} \right) \rho = u\rho.$$

We now model the linear attenuation coefficient as a linear combination of basis materials:

$$\mu(E) = u_1\rho_1 + u_2\rho_2 + \dots + u_N\rho_N,$$

where N is the number of basis materials.

Generalized linear model of multi-energy CT in image space

Let us assume that we are imaging with M discrete X-ray energies. The forward model is now

$$\begin{aligned}\mu_1 &= u_{11}\rho_1 + u_{12}\rho_2 + \dots + u_{1N}\rho_N \\ \mu_2 &= u_{21}\rho_1 + u_{22}\rho_2 + \dots + u_{2N}\rho_N \\ &\vdots \\ \mu_M &= u_{M1}\rho_1 + u_{M2}\rho_2 + \dots + u_{MN}\rho_N,\end{aligned}$$

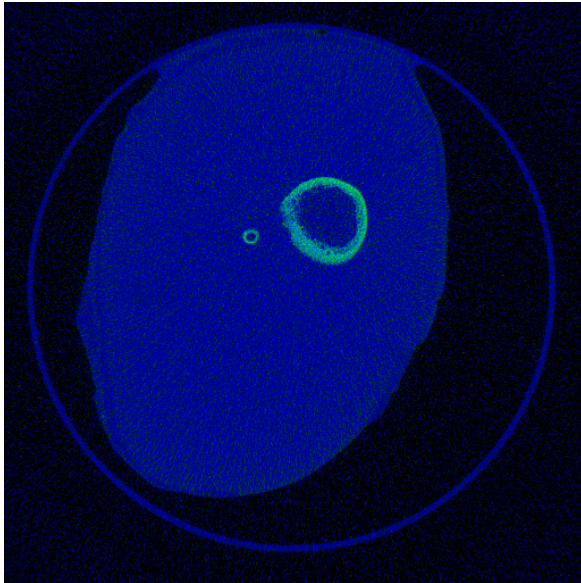
or in a matrix form

$$\mathbf{x} = \mathbf{U}\boldsymbol{\rho}.$$

Usually practice dictates that the inverse model must be limited to two energies and two energies, *i.e.*, dual-energy CT (DECT):

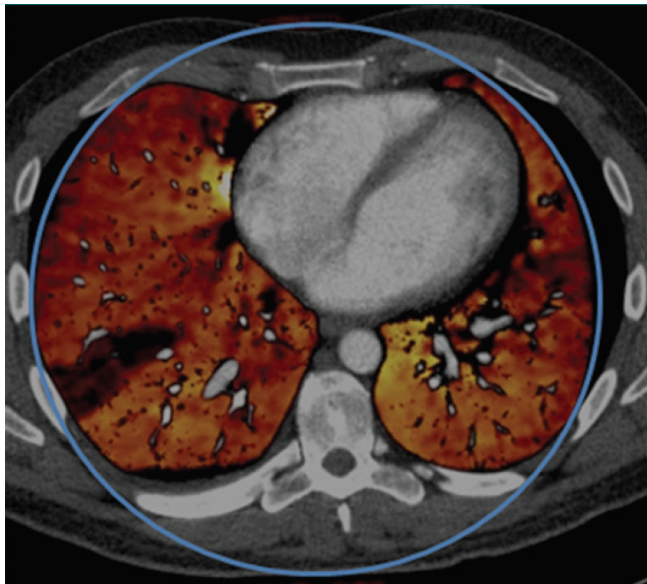
$$\mathbf{x} = \mathbf{U}_d\boldsymbol{\rho} = \begin{pmatrix} u_{11} & u_{12} \\ u_{21} & u_{22} \end{pmatrix} \begin{pmatrix} \rho_1 \\ \rho_2 \end{pmatrix}.$$

Material decomposition example: chicken leg, water and bone bases



Material decomposition codes courtesy of [Mikael Juntunen](#), University of Oulu

Clinical example of material decomposition: detection of a pulmonary embolism



McCollough
et al., 2015

Outline

X-ray physics and imaging model in computed tomography

Material decomposition in multi-energy CT

Joint reconstruction in multi-energy CT

FIPS open datasets and Industrial Mathematics CT
Laboratory at the University of Helsinki

General principle of iterative reconstruction using regularization

Let us define the objective function

$$F(x) = \|Ax - m\|_2^2 + \alpha W(x),$$

where the regularization function $W(x)$ is used to incorporate *a priori* information into the solution. $\alpha \in \mathbb{R}_+$ is the regularization parameter.

We now seek to obtain the reconstruction

$$\tilde{f}(m) = \arg \min_{x \in \mathbb{R}^n} \{ \|Ax - m\|_2^2 + \alpha W(x) \}.$$

Reconstruction in multi-energy CT

We now seek to find a set of solution x_1, x_2, \dots, x_n , where n is the number of measurements at different energies.

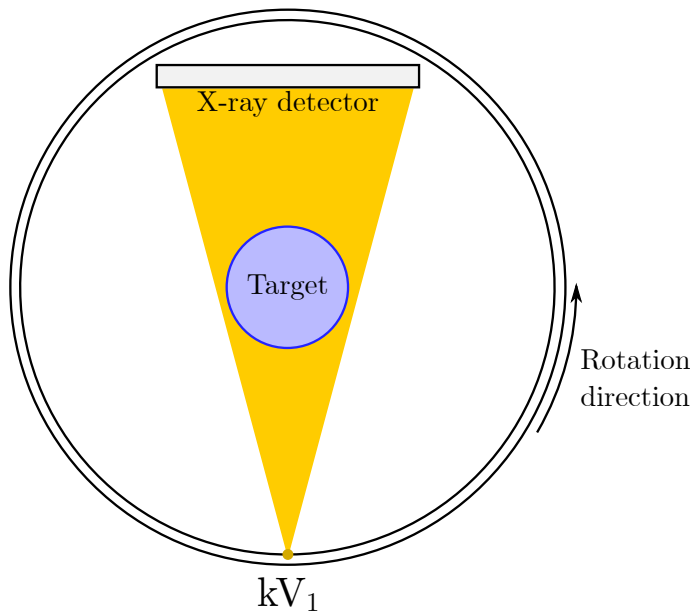
Assumption: *the energy dependence of x_n will lead to solutions that differ in contrast but remain structurally similar.*

Reconstruction in multi-energy CT

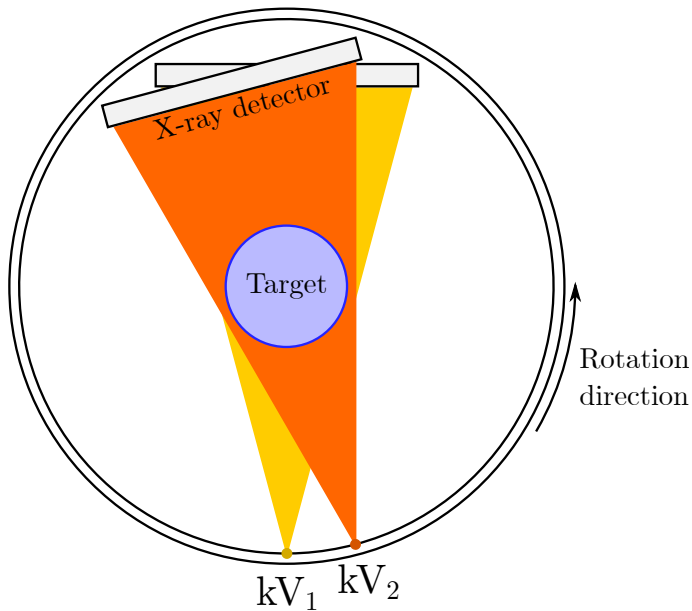
Motivation: *develop a reconstruction technique for low-dose multi-energy CT that is robust enough for quantitative analysis.*

We tested 7 different reconstruction schemes for *sparse projection multi-energy CT* using real X-ray measurement data.

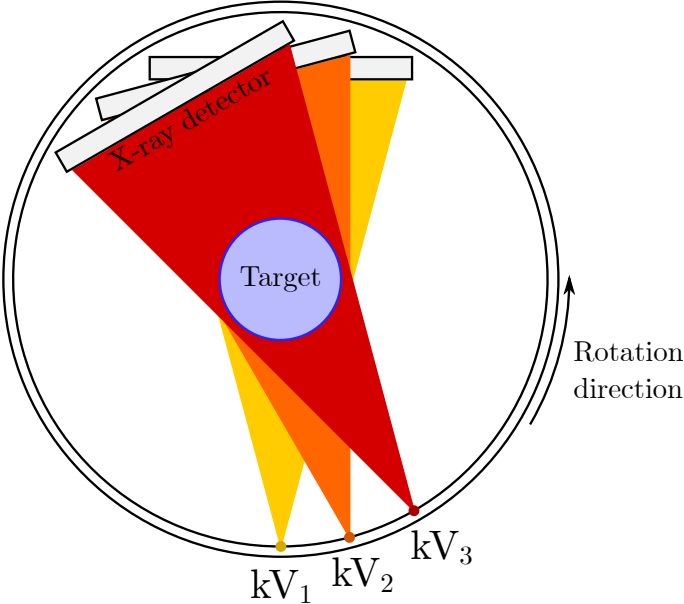
Measurement geometry



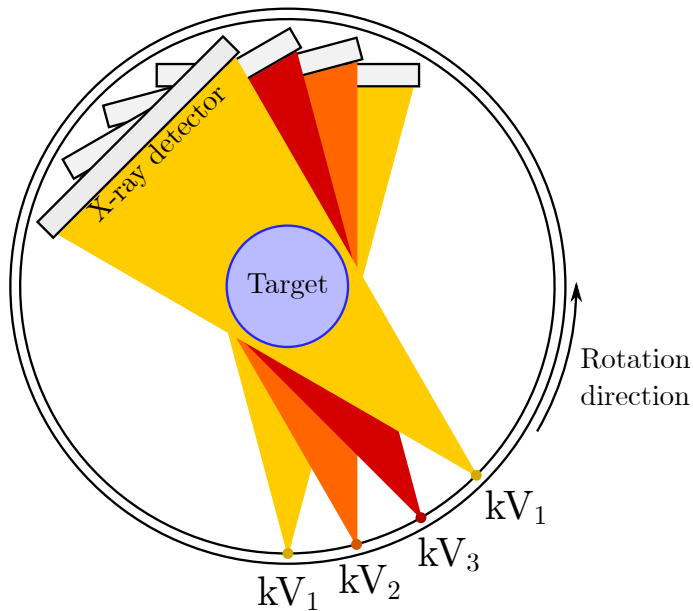
Measurement geometry



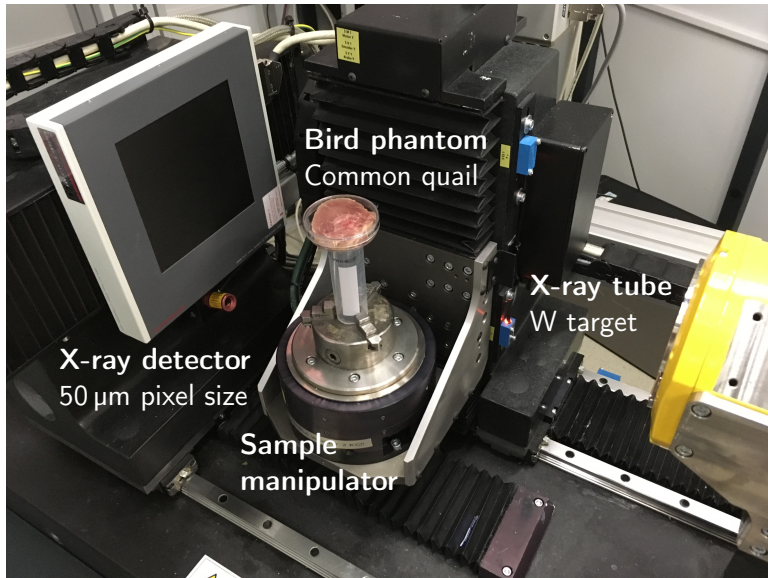
Measurement geometry



Measurement geometry



Multi-energy CT Measurements: GE Nanotom 180F at Dept. of Physics, UH



Bird phantom measurements

We acquired 720 projections at each energy and selected 30 projections for each:

$$E_1 : 0^\circ, 12^\circ, 24^\circ \dots, 348^\circ$$

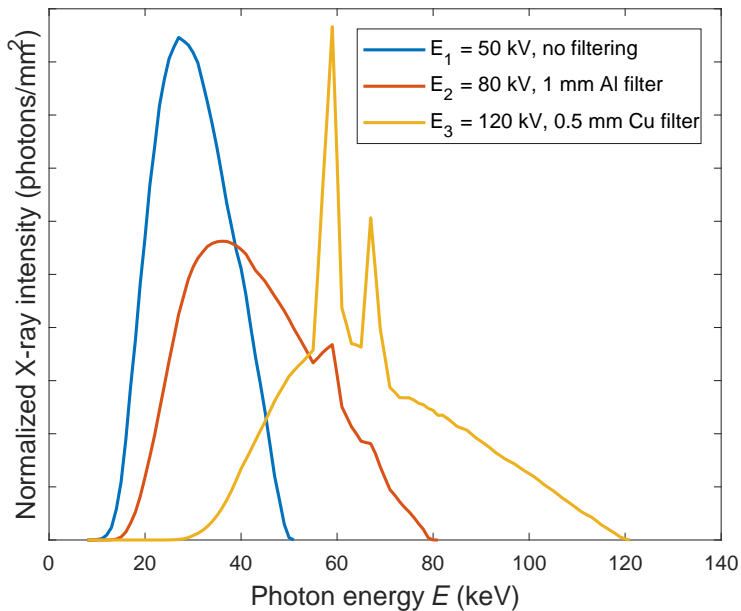
$$E_2 : 4^\circ, 16^\circ, 28^\circ, \dots, 352^\circ$$

$$E_3 : 8^\circ, 20^\circ, 32^\circ, \dots, 356^\circ$$

We used the ASTRA Tomography Toolbox to create our forward model and to compute reference reconstructions (FBP, Shepp-Logan filter, 720 projections).

www.astra-toolbox.com

X-ray spectra used in measurements



No prior

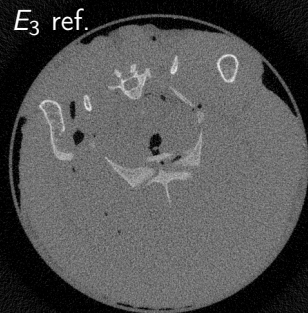
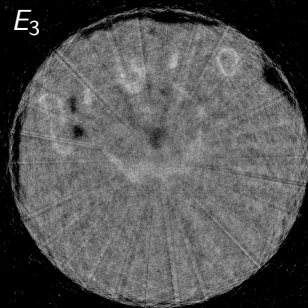
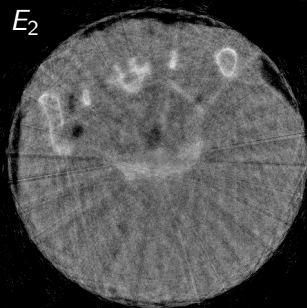
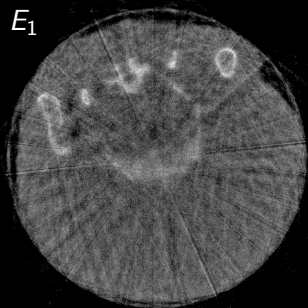
We define the regularization function as

$$W(x) = 0.$$

(Only non-negativity constraint.)

The images are estimated separately for each energy.

No prior



Total variation (TV)

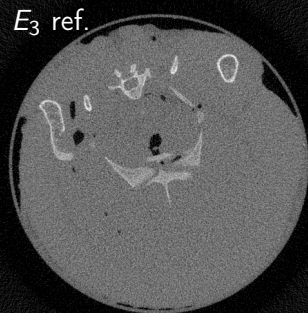
We define the regularization function as

$$W(x) = \int_{\Omega} (\|\nabla x\|^2 + \beta^2)^{1/2}.$$

TV favors sparsity of the gradient, *i.e.*, flat areas in x .

The images are estimated separately for each energy.

Total variation (TV)



Joint total variation (JTV)

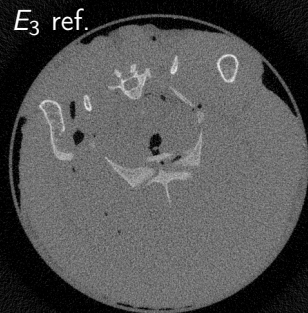
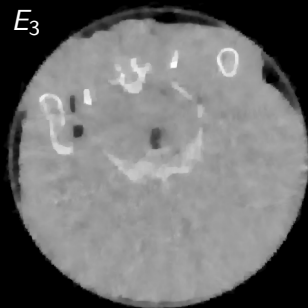
We define the regularization function as

$$W(x_1, x_2, x_3) = \int_{\Omega} (\|\nabla x_1\|^2 + \|\nabla x_2\|^2 + \|\nabla x_3\|^2 + \beta^2)^{1/2}.$$

JTV favors sparsity of joint gradient, *i.e.*, nonzero gradients at the same locations.

The images for different energies are estimated simultaneously.

Joint total variation (JTV)



Second difference (D2)

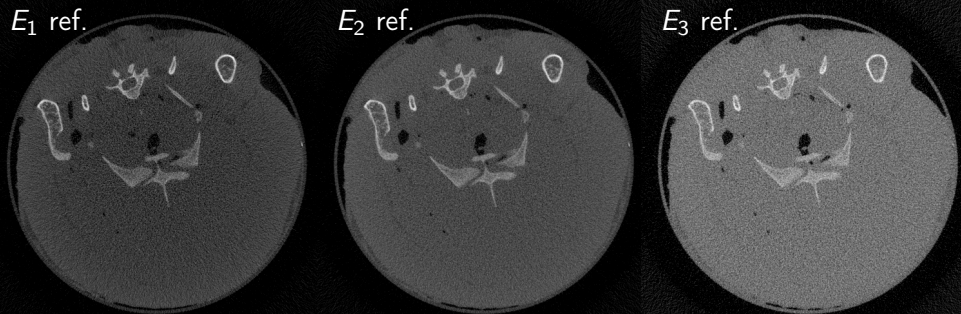
We define the regularization function as

$$W(x_1, x_2, x_3) = \int_{\Omega} (\|x_3 - 2x_2 + x_1\|^2).$$

D2 favors reconstructions that change linearly in the energy direction.

The images for different energies are estimated simultaneously.

Second difference (D2)



Structural prior (S)

We use the structural similarity function

$$S_i(x_1, x_2) = \frac{\sigma_{x_1 x_2} + C}{\sigma_{x_1} \sigma_{x_2} + C},$$

where the cross correlation $\sigma_{x_1 x_2}$ and the standard deviations σ_{x_1} and σ_{x_2} , and S_i are computed locally using a 11x11 window that moves pixel by pixel over the entire image.

The final structure part is the mean of the local structure values

$$S = \frac{1}{M} \sum_{i=1}^M S_i.$$

Structural prior (S)

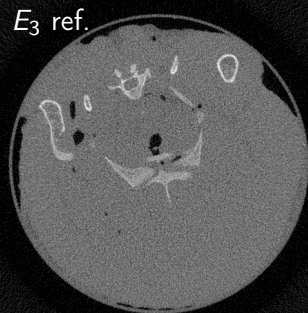
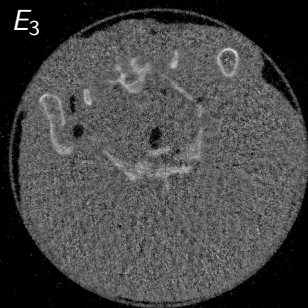
We now define the regularization function as

$$W(x_1, x_2, x_3) = \frac{1}{S(x_1, x_2, x_3)},$$

where the structure parts are computed in pairs with

$$S(x_1, x_2, x_3) = S(x_1, x_2) + S(x_2, x_3) + S(x_3, x_1).$$

Structural prior (S)

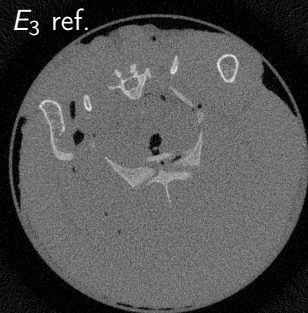


Second difference + total variation (D2+TV)

We now define the objective function as

$$\begin{aligned} F(x) = & \|Ax - m\|_2^2 + \alpha_{D2} \int_{\Omega} (\|x_3 - 2x_2 + x_1\|^2) \\ & \alpha_1 \int_{\Omega} (\|\nabla x_1\|^2 + \beta^2)^{1/2} + \\ & \alpha_2 \int_{\Omega} (\|\nabla x_2\|^2 + \beta^2)^{1/2} + \\ & \alpha_3 \int_{\Omega} (\|\nabla x_3\|^2 + \beta^2)^{1/2}. \end{aligned}$$

Second difference + total variation (D2+TV)

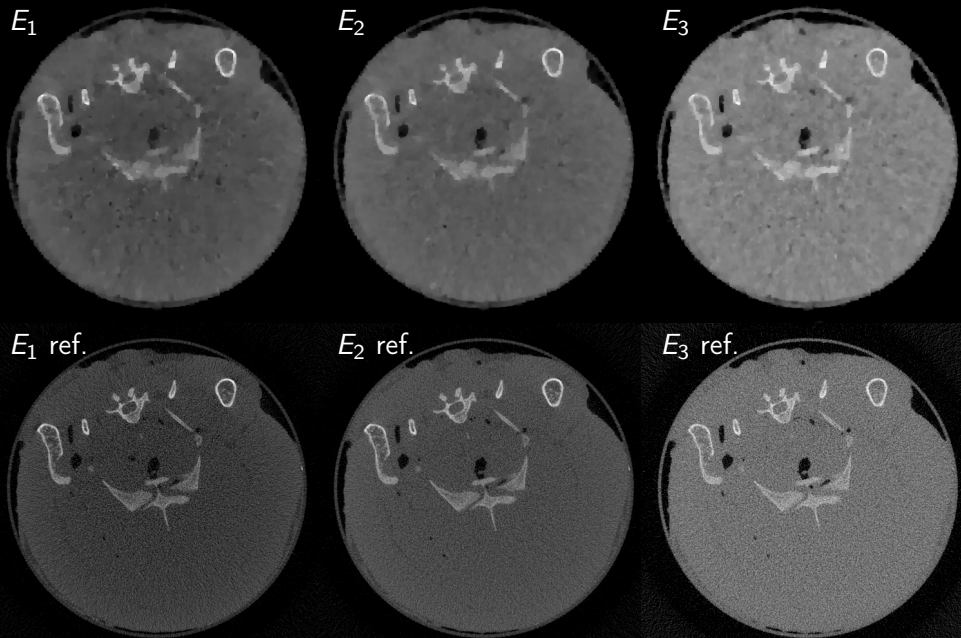


Structural prior + total variation (S+TV)

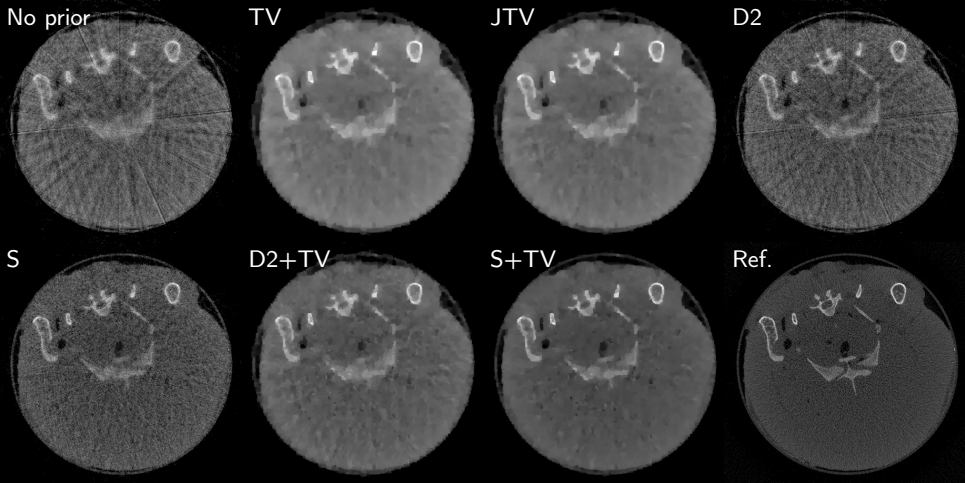
We now define the objective function as

$$F(x) = \|Ax - m\|_2^2 + \alpha_S \frac{1}{\mathcal{S}(x_1, x_2, x_3)} \\ \alpha_1 \int_{\Omega} (\|\nabla x_1\|^2 + \beta^2)^{1/2} + \\ \alpha_2 \int_{\Omega} (\|\nabla x_2\|^2 + \beta^2)^{1/2} + \\ \alpha_3 \int_{\Omega} (\|\nabla x_3\|^2 + \beta^2)^{1/2}.$$

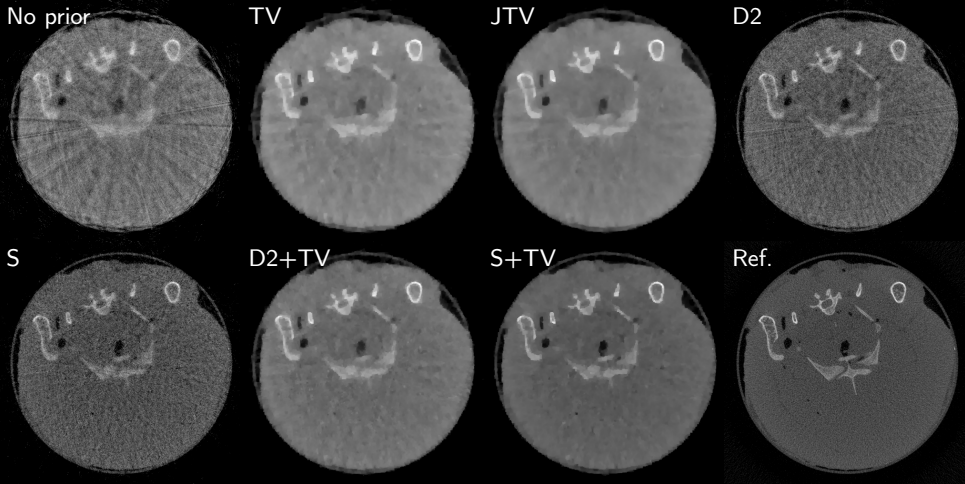
Structural prior + total variation (S+TV)



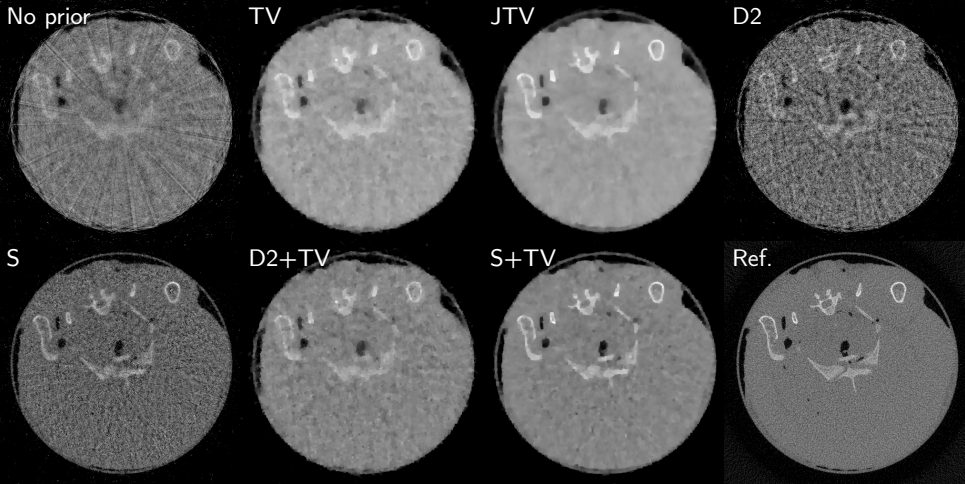
Comparison of methods: E_1 reconstructions



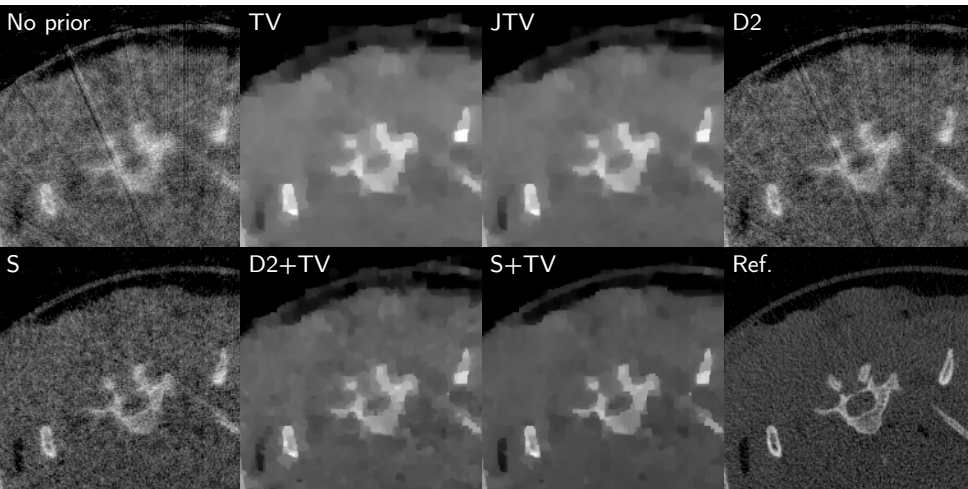
Comparison of methods: E_2 reconstructions



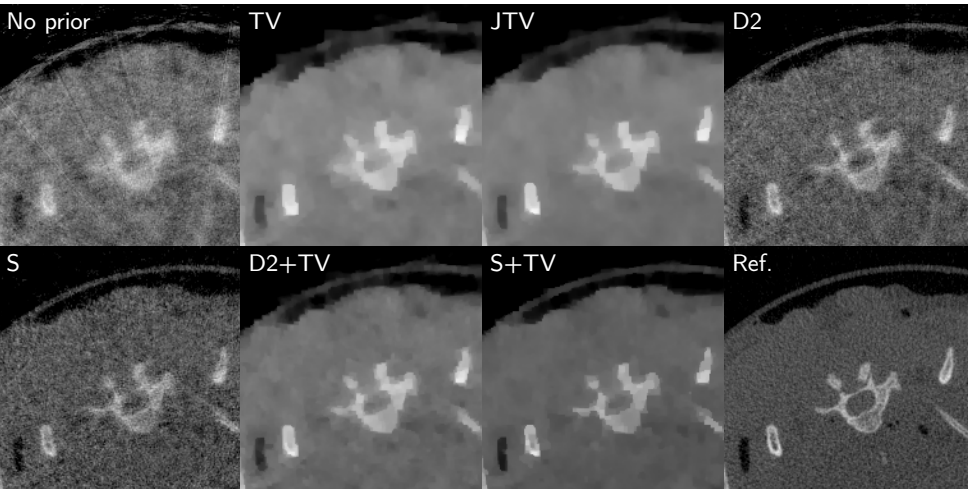
Comparison of methods: E_3 reconstructions



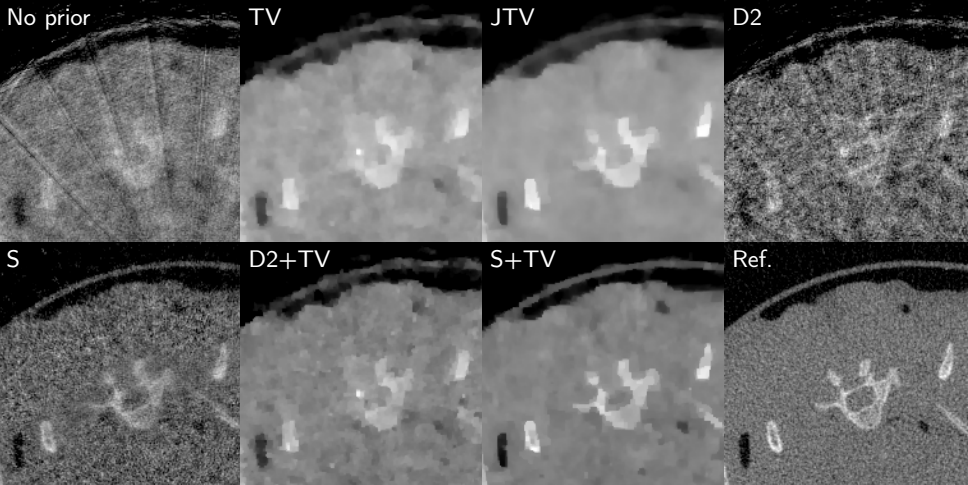
Comparison of methods: E_1 reconstructions, closeup



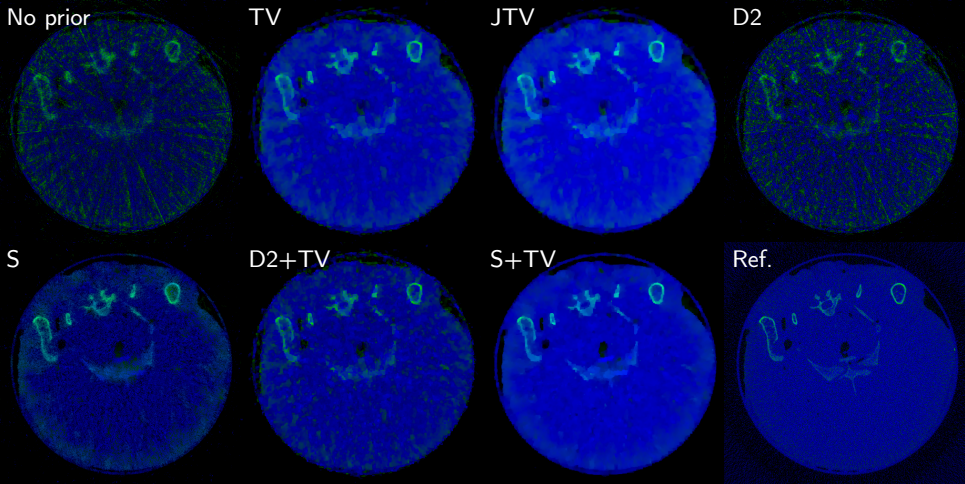
Comparison of methods: E_2 reconstructions, closeup



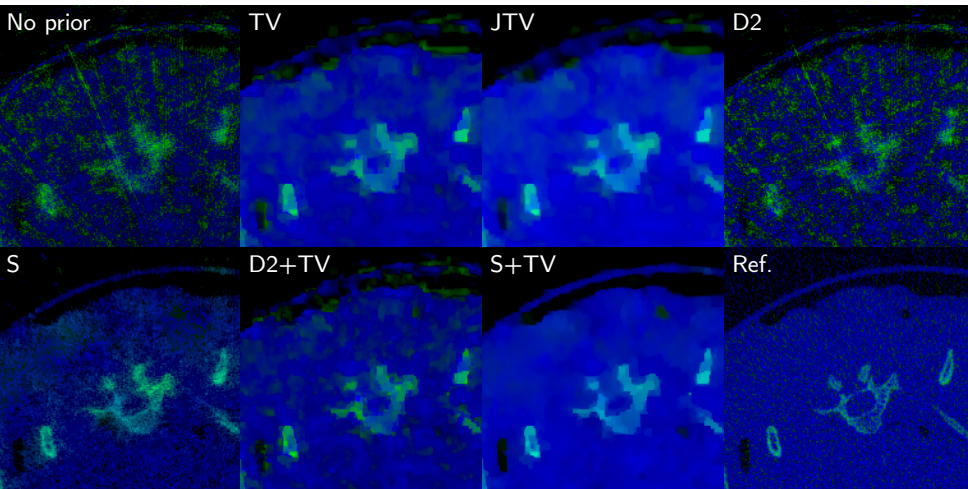
Comparison of methods: E_3 reconstructions, closeup



Comparison of methods: material decomposition into water and bone bases



Comparison of methods: material decomposition into water and bone bases



Joint Reconstruction in Low Dose Multi-Energy CT

Jussi Toivanen^{*}, Alexander Meaney^{**}, Samuli Siltanen^{**} and Ville
Kolehmainen^{*}

^{*}Department of Applied Physics, University of Eastern Finland,
POB 1627, FI-70211 Kuopio, Finland

^{**}Department of Mathematics and Statistics, University of
Helsinki, Finland

April 12, 2019

Abstract

Multi-energy CT takes advantage of the non-linearly varying attenuation properties of elemental media with respect to energy, enabling more precise material identification than single-energy CT. The increased precision comes with the cost of a higher radiation dose. A straightforward way to lower the dose is to reduce the number of projections per energy, but this makes tomographic reconstruction more ill-posed. In this paper, we propose how this problem can be

What next?

Utilize the third energy bin for more basis materials.

Extend our method to **3D**.

Larger testing with new datasets.

Establish a quantitative evaluation of reconstruction quality.

Will the method yield advantages for PCD imaging?

What is the optimal way to choose the regularization parameter?

Outline

X-ray physics and imaging model in computed tomography

Material decomposition in multi-energy CT

Joint reconstruction in multi-energy CT

**FIPS open datasets and Industrial Mathematics CT
Laboratory at the University of Helsinki**

FIPS open datasets

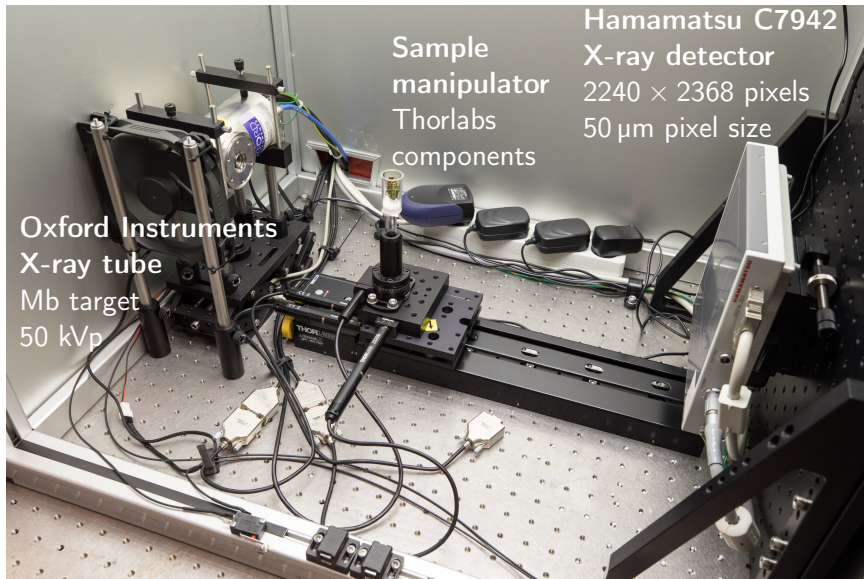
The Finnish Inverse Problems Society provides open access datasets of real X-ray tomographic data at <http://www.fips.fi/dataset.php>.

MATLAB codes and computational resources are available at the FIPS Computational Blog: <https://blog.fips.fi>.



Industrial Mathematics

Computed Tomography Laboratory



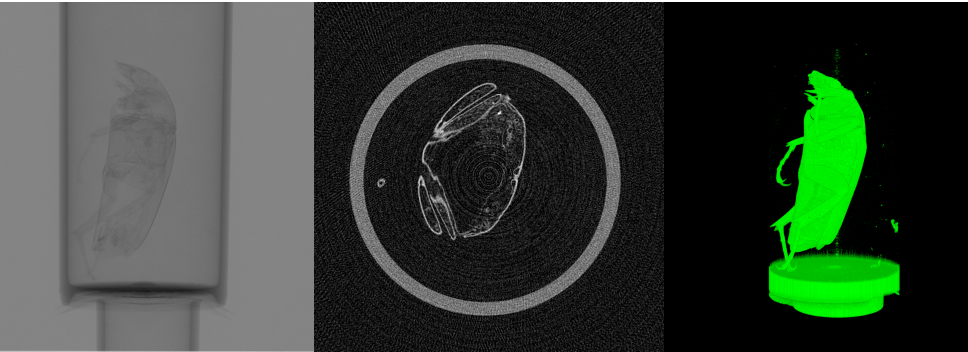
Oxford Instruments
X-ray tube
Mb target
50 kVp

Sample
manipulator
Thorlabs
components

Hamamatsu C7942
X-ray detector
2240 × 2368 pixels
50 μm pixel size

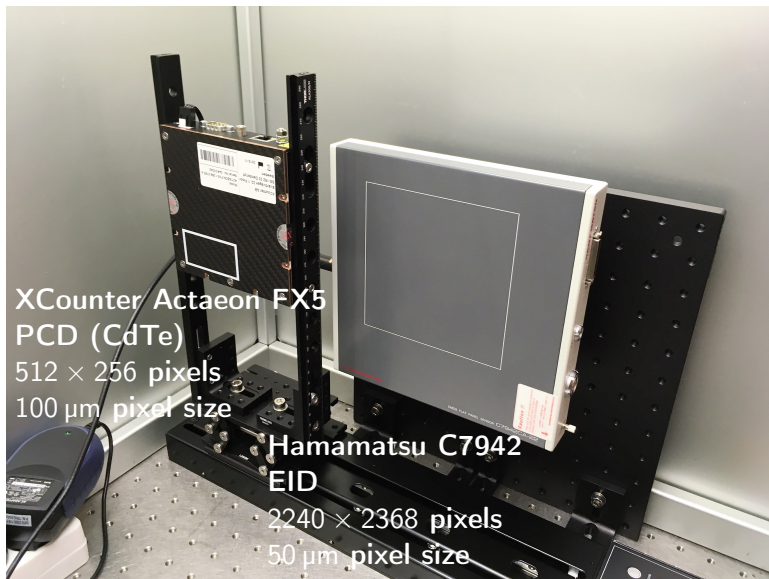
Industrial Mathematics

Computed Tomography Laboratory



Stephanorrhina guttata, common name Spotted Flower Beetle

Teaser: new micro-CT laboratory under construction



Thank you for your attention!



Selected bibliography

Chen, Zhang, Sidky, Xia and Pan 2017

Ding, Niu, Zhang and Long 2018

Ehrhardt et al. 2014, 2016

Gao, Yu, Osher and Wang 2011

Kazantsev et al 2018

Niu, Yu, Ma and Wang 2018

Rigie and La Riviere 2015

Rigie, Sanchez and La Riviere 2017

Semerci, Hao, Kilmer and Miller 2014

Wu, Zhang, Wang, Liu, Chen and Yu 2018

Yang, Cong and Wang 2017

Zhang, Mou, Wang and Yu 2017